

Proceedings of the Institution of Mechanical Engineers, Part L: Journal of Materials Design and Applications

<http://pil.sagepub.com/>

Structural efficiency maps for beams subjected to bending

D Pasini, D J Smith and S C Burgess

Proceedings of the Institution of Mechanical Engineers, Part L: Journal of Materials Design and Applications 2003
217: 207

DOI: 10.1177/146442070321700303

The online version of this article can be found at:

<http://pil.sagepub.com/content/217/3/207>

Published by:



<http://www.sagepublications.com>

On behalf of:



[Institution of Mechanical Engineers](http://www.institutionofmechanicalengineers.org)

Additional services and information for *Proceedings of the Institution of Mechanical Engineers, Part L: Journal of Materials Design and Applications* can be found at:

Email Alerts: <http://pil.sagepub.com/cgi/alerts>

Subscriptions: <http://pil.sagepub.com/subscriptions>

Reprints: <http://www.sagepub.com/journalsReprints.nav>

Permissions: <http://www.sagepub.com/journalsPermissions.nav>

Citations: <http://pil.sagepub.com/content/217/3/207.refs.html>

>> [Version of Record](#) - Jul 1, 2003

[What is This?](#)

Structural efficiency maps for beams subjected to bending

D Pasini*, D J Smith and S C Burgess

Department of Mechanical Engineering, University of Bristol, Bristol, UK

Abstract: The structural efficiency of different cross-sections subjected to bending is considered in this paper. An envelope efficiency parameter, λ , is defined in terms of two shape transformers, ψ_A and ψ_I . These transformers describe the relative ratio of the area and the second moment of area of the cross-sectional shape with respect to a rectangular envelope surrounding the shape. It is shown in a structural efficiency map that the mass efficiency of all cross-sectional shapes subjected to bending is bounded by two limiting curves. One limit curve represents cross-sections with material as far as possible from the neutral axis, the other limit curve is for cross-sections with material close to the neutral axis. The application of the map to two practical cases is also considered, together with scaling of the rectangular envelope.

Keywords: structural efficiency, optimal shape, shape selection

NOTATION

| | |
|-----------|---|
| A | cross-sectional area |
| b | internal width (m) |
| B | width (m) |
| E | Young's modulus (GPa) |
| h | internal height (m) |
| H | height (m) |
| I | second moment of area (m ⁴) |
| L | length (m) |
| p | performance criterion |
| r_g | radius of gyration (m) |
| λ | envelope efficiency parameter |
| ρ | material density (mg/m ³) |
| ψ | shape transformer |

1 INTRODUCTION

The minimization of mass is very often an important issue in structural design. Lightweight structures help to achieve lower material cost and environmental impact and provide high performance such as low inertial loads and high natural frequency. These features are often required in many branches of engineering.

The MS was received on 4 October 2002 and was accepted after revision for publication on 26 March 2003.

**Corresponding author: Department of Mechanical Engineering, University of Bristol, Queen's Building, University Walk, Bristol BS8 1TR, UK.*

Selecting efficient cross-sectional shapes is one well-founded way to reduce the mass of a structure. Several methods for assessing the efficiency of cross-sectional shapes have been developed in the last century. Cox [1] considered the effect of shapes on the selection of different structures. However, Shanley [2] first introduced a systematic method to take into account the geometric properties of shapes for the selection of light structures. He proposed a shape parameter that is governed by the shape of the cross-section. In more recent years, Parkhouse [3, 4] proposed a dilution factor to describe the geometrical property relationship between different cross-sections and their representative solid sections. Similarly, Ashby [5] suggested a method to assess the structural performance of cross-sections using shape factors and material indices and also showed that visualizing the problem graphically helps to obtain insight. Although the methodology is mainly applicable where there are no dimensional restrictions, the case of height- or width-constrained beams was addressed by Ashby [6], and his theory was used by Burgess [7] to discuss the effects of height constraints on structural efficiency. However, only recently a general theory of modelling the structural efficiency of cross-sections scaled in any arbitrary direction was presented [8, 9]. These studies have shown that a generic geometrical constraint, which imposes restrictions to the scaling of cross-sections, has an important effect on what are the best material and/or shape for a particular application.

In this paper, structural efficiency maps are developed for beams subjected to bending. These maps are used to explore how a rectangular design space, defined by its height and width, is efficiently occupied by shapes whose principal

dimensions touch the boundaries of the design space. The novel feature of this work is the definition of an envelope efficiency parameter, λ . The method allows direct visual comparison of the performance of different shapes. The efficiency maps are used to assess the relative performance of currently available standard cross-sections. The maps are also used to plot the performance of layered systems such as those previously described by Smith and Partridge [10]. Finally, the analysis is applied to cross-sections that are arbitrarily scaled, that is, enlarged or contracted in any direction including widthwise, heightwise, proportionally and in any other direction.

2 RELEVANT GEOMETRIC PROPERTIES

This section describes the geometric properties that are relevant to examine the efficiency of beams. In bending stiffness design, the structures are designed to be as light as possible for a given stiffness requirement and span. Expressions for the mass, m , and the bending stiffness, k , of a structure are

$$m = \rho AL \quad (1)$$

$$k = c_1 \frac{EI}{L^3} \quad (2)$$

where c_1 is a constant depending on boundary and loading conditions applied to a beam subjected to bending, ρ is the density, E is the Young's modulus, L is the span and A and I are the area and second moment of area of the cross-sections respectively.

The minimum weight or performance criterion, p , for the selection of structures, which maximizes the stiffness while minimizing the mass, is the ratio of equations (2) and (1)

$$p = \frac{k}{m} = \frac{c_1 E I}{L^4 \rho A} \quad (3)$$

Expressions (1) to (3) show that the geometrical properties relevant to the efficiency of cross-sections are the area and the second moment of area. It may be convenient to represent the second moment of area in terms of radius of gyration, noting that r_g is defined as $r_g = \sqrt{I/A}$.

3 THEORY OF MODELLING THE GEOMETRIC PROPERTIES OF SHAPES

The cross-section is defined as having shape and an envelope. The envelope is described by the main dimensions of the cross-section. Within the envelope there is a shape. Figure 1 shows two examples. The width and depth of the envelope define the extremities of the cross-section shape. The elliptical cross-section in Fig. 1a belongs to a class of specific shapes, while the cross-section in Fig. 1b is a general case.

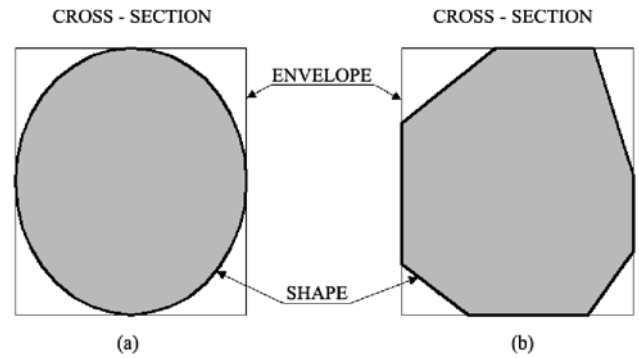


Fig. 1 Envelope and shape: the size of the envelope and the type of shape make a cross-section

The following definitions are adopted to distinguish the content of the cross-section, i.e. the shape, from its envelope (these definitions are consistent with those used in earlier papers [8, 9]):

For a generic cross-section

I = second moment of area

A = area of shape

r_g = radius of gyration

For the shape envelope

B, H = width and height

I_D = second moment of area of the envelope

A_D = area of the envelope

r_{gD} = radius of gyration of the envelope

Expressions for area, second moment of area and radius of gyration of common cross-sections have been derived. These expressions are shown in Table 1, where B and H are the width and depth of the envelope and b and h are the internal width and height of hollow cross-sections.

The area and second moment of area of a cross-section and its envelope can be related by defining two geometric shape transformers, ψ_A and ψ_I , as

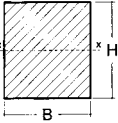
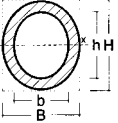
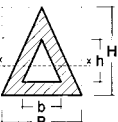
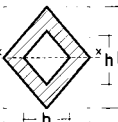
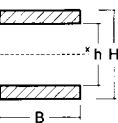
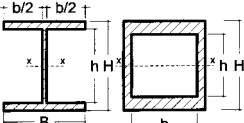
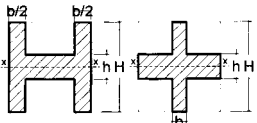
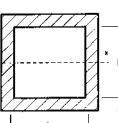
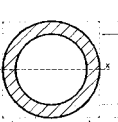
$$\begin{aligned} \psi_A &= \frac{A}{A_D} \\ \psi_I &= \frac{I}{I_D} \end{aligned} \quad (4)$$

The envelope efficiency parameter of a cross-section, λ , is now introduced. This parameter describes how efficiently the area of a cross-sectional shape is placed in its envelope. The parameter is defined as

$$\lambda = \frac{\psi_I}{\psi_A} = \frac{r_g^2}{r_{gD}^2} \quad (5)$$

Expressions for ψ_I , ψ_A and λ are given in Table 2. For a rectangular cross-section, its dimensions coincide with the

Table 1 Area, second moment of area and radius of gyration of the most common sections.
Note that $B = H$ in the last two rows is only for square boxes and circular tubes

| CROSS-SECTIONAL SHAPE | Area A | Second moment of Area about x-x I | Radius of gyration $r_g^2 = \frac{I}{A}$ |
|---|----------------------------|---|---|
|  | BH | $\frac{BH^3}{12}$ | $\frac{H^2}{12}$ |
|  | $\frac{\pi}{4}(BH - bh)$ | $\frac{\pi}{64}(BH^3 - bh^3)$ | $\frac{1}{16} \left(\frac{BH^3 - bh^3}{BH - bh} \right)$ |
|  | $\frac{1}{2}(BH - bh)$ | $\frac{(BH^3 - bh^3)}{36}$ | $\frac{1}{18} \left(\frac{BH^3 - bh^3}{BH - bh} \right)$ |
|  | $\frac{1}{2}(BH - bh)$ | $\frac{(BH^3 - bh^3)}{48}$ | $\frac{1}{24} \left(\frac{BH^3 - bh^3}{BH - bh} \right)$ |
|  | $B(H - h)$ | $\frac{B(H^3 - h^3)}{12}$ | $\frac{H^2}{12} \left(1 + \frac{h}{H} + \frac{h^2}{H^2} \right)$ |
|  | $BH - bh$ | $\frac{BH^3 - bh^3}{12}$ | $\frac{1}{12} \left(\frac{BH^3 - bh^3}{BH - bh} \right)$ |
|  | $bH + h(B - b)$ | $\frac{bH^3}{12} + \frac{(B - b)h^3}{12}$ | $\frac{1}{12} \left(\frac{bH^3 + (B - b)h^3}{bH + (B - b)h} \right)$ |
|  | $H^2 - h^2$ | $\frac{H^4 - h^4}{12}$ | $\frac{H^2 + h^2}{12}$ |
|  | $\frac{\pi}{4}(H^2 - h^2)$ | $\frac{\pi}{64}(H^4 - h^4)$ | $\frac{H^2 + h^2}{16}$ |

envelope, and consequently the geometric transformers, ψ_I and ψ_A , and the envelope efficiency parameter, λ , are unity

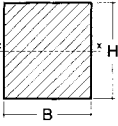
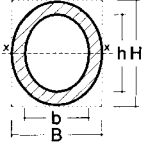
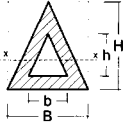
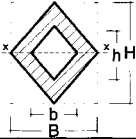
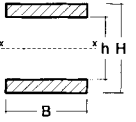
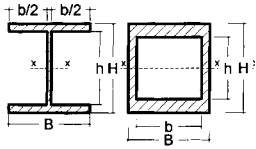
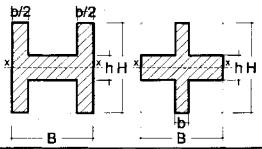
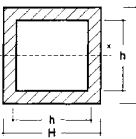
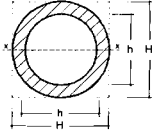
$$A = A_D \rightarrow \psi_A = 1$$

$$I = I_D \rightarrow \psi_I = 1$$

$$r_g = r_{gD} \rightarrow \lambda = 1$$

where ψ_I , ψ_A and λ are dimensionless design parameters that describe the geometric quantities and the efficiency of a generic cross-section in relation to its envelope. They can be used in a design task quickly to identify and distinguish the contribution to the structural efficiency of the shape from its envelope [11].

Table 2 Geometric shape transformers, ψ_I and ψ_A , and envelope efficiency parameter, λ , of sections. Note that $B = H$ in the last two rows is only for square boxes and circular tubes

| CROSS-SECTIONAL SHAPE for the same envelope | $\psi_A = \frac{A}{A_D}$ | RANGE ψ_A | $\psi_I = \frac{I}{I_D}$ | RANGE ψ_I | $\lambda = \frac{\psi_I}{\psi_A}$ | RANGE λ |
|---|---|-------------------|---|-------------------|---|--------------------|
| Envelope A_D, I_D  | 1 | No range | 1 | No range | 1 | No range |
|  | $\frac{\pi}{4} \left(1 - \frac{bh}{BH}\right)$ | 0 to $\pi/4$ | $\frac{3\pi}{16} \left(1 - \frac{bh^3}{BH^3}\right)$ | 0 to $3\pi/16$ | $\frac{3}{4} \left(\frac{1 - \frac{bh^3}{BH^3}}{1 - \frac{bh}{BH}} \right)$ | 3/4 to 9/4 |
|  | $\frac{1}{2} \left(1 - \frac{bh}{BH}\right)$ | 0 to 1/2 | $\frac{1}{3} \left(1 - \frac{bh^3}{BH^3}\right)$ | 0 to 1/3 | $\frac{2}{3} \left(\frac{1 - \frac{bh^3}{BH^3}}{1 - \frac{bh}{BH}} \right)$ | 2/3 to 2 |
|  | $\frac{1}{2} \left(1 - \frac{bh}{BH}\right)$ | 0 to 1/2 | $\frac{1}{4} \left(1 - \frac{bh^3}{BH^3}\right)$ | 0 to 1/4 | $\frac{1}{2} \left(\frac{1 - \frac{bh^3}{BH^3}}{1 - \frac{bh}{BH}} \right)$ | 1/2 to 3/2 |
|  | $1 - \frac{h}{H}$ $\frac{b}{B} \left(1 - \frac{h}{H}\right)$ | 0 to 1 | $1 - \frac{h^3}{H^3}$ $\left(1 - \frac{h^3}{H^3}\right) \frac{b}{B}$ | 0 to 1 | $1 + \frac{h}{H} + \frac{h^2}{H^2}$ | 1 to 3 |
|  | $1 - \frac{bh}{BH}$ | 0 to 1 | $1 - \frac{bh^3}{BH^3}$ | 0 to 1 | $\frac{1 - \frac{bh^3}{BH^3}}{1 - \frac{bh}{BH}}$ | 1 to 3 |
|  | $\frac{b}{B} + \frac{h}{H} - \frac{bh}{BH}$ | 0 to 1 | $\frac{b}{B} + \frac{h^3}{H^3} - \frac{bh^3}{BH^3}$ | 0 to 1 | $\frac{\frac{b}{B} + \frac{h^3}{H^3} - \frac{bh^3}{BH^3}}{\frac{b}{B} + \frac{h}{H} - \frac{bh}{BH}}$ | 0 to 1 |
|  | $1 - \frac{h^2}{H^2}$ | 0 to 1 | $1 - \frac{h^4}{H^4}$ | 0 to 1 | $1 + \frac{h^2}{H^2}$ | 1 to 2 |
|  | $\frac{\pi}{4} \left(1 - \frac{h^2}{H^2}\right)$ | 0 to $\pi/4$ | $\frac{3\pi}{16} \left(1 - \frac{h^4}{H^4}\right)$ | 0 to $3\pi/16$ | $\frac{3}{4} \left(1 + \frac{h^2}{H^2}\right)$ | 3/4 to 3/2 |

For a given class of cross-sectional shape within an envelope there is a theoretical range of values for the parameters ψ_I , ψ_A and λ . For example, consider the case of a hollow elliptical cross-section. The lowest value of ψ_A is zero, and this corresponds to an infinitesimally

thin wall thickness for the cross-section. The largest value of ψ_A is $\pi/4$ and occurs when the elliptical cross-section is solid. Theoretical ranges for the parameters ψ_I , ψ_A and λ for other different cross-sections are shown in Table 2.

In the following sections, the geometric parameters defined here are substituted into equation (3) to derive an expression of the performance criterion function only of the shape transformers. Firstly a performance criterion and then an efficiency map are described.

4 ENVELOPE EFFICIENCY MAPS

4.1 Performance criterion

To establish the performance criterion of the cross-section for beams subjected to bending, consider two beams of the same material. One beam has a rectangular cross-section that completely fills its rectangular envelope and is consequently called the reference beam. The efficiency p of the reference beam is p_0 , and it is given by equation (3) so that

$$p_0 = \frac{c_1 E I_D}{L^4 \rho A_D} \quad (6)$$

The ratio of the performance criterion of the second beam relative to the reference beam is

$$\frac{p}{p_0} = \frac{I A_D}{I_D A} = \frac{\psi_I}{\psi_A} = \lambda \quad (7)$$

When the envelope is completely filled, $p = p_0$ and $\psi_I = \psi_A = \lambda = 1$. When only partially occupied, ψ_I and

ψ_A are less than 1, as indicated in Table 2. The variation in the performance criterion ratio $p/p_0 = \lambda$ can also be illustrated for various cross-sectional shapes by examining the variations in the shape transformers ψ_I and ψ_A . This is presented in the next section.

4.2 Envelope efficiency map

Using equation (7) and the expressions for ψ_I and ψ_A , given in Table 2, results for λ are plotted in Fig. 2. Within the range defined by ψ_I plotted as a function of ψ_A there are two limiting curves, curves 1 and 2. Within the curves 1 and 2 there exist all geometric cross-sectional shapes that partially fill the envelope defined by B and H . Furthermore, there are no cross-sectional shapes within the envelope $B \times H$ subjected to bending that are outside the boundaries defined by the curves 1 and 2.

Curve 1 represents the conditions where the upper and lower outside surfaces of the beam are occupied by material. This is the case of an I-beam with an infinitely thin vertical web with the dimensions $B - b$ tending to zero (see Table 2) or a layered system with the centre filled with material of very low Young's modulus relative to the outside material.

Curve 2 represents a rather idealized case of an I-section beam turned on its side (e.g. an H-section). The outer sides of the H are infinitely thin (with the dimension b tending to zero), with the centre cross-member increasing with thickness with increasing ψ_I and ψ_A . It should be noted that for

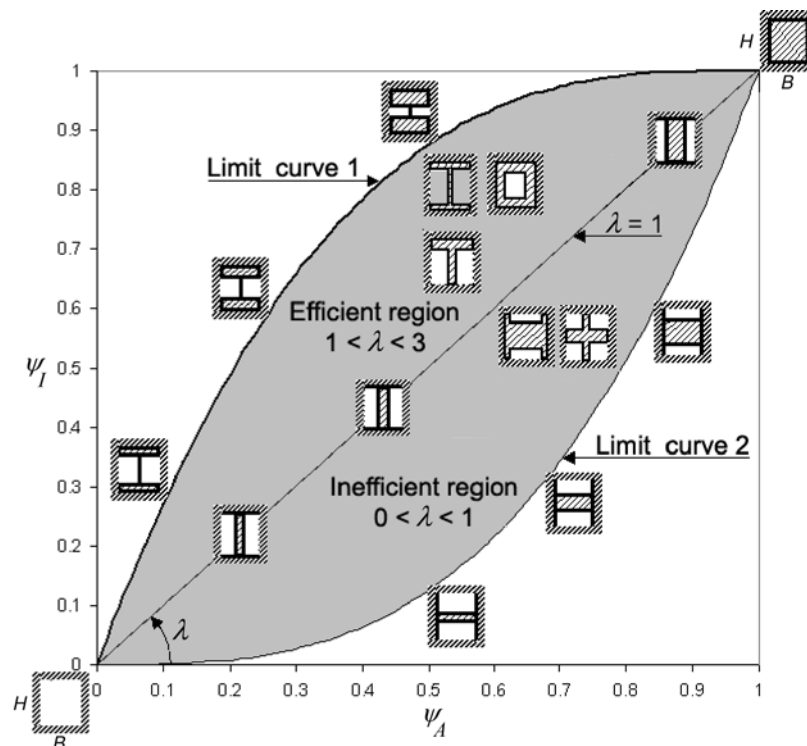


Fig. 2 Rectangle efficiency map: the grey region represents the complete domain of cross-sectional shapes with the same envelope. The domain is split into efficient and inefficient regions according to λ

both curves 1 and 2 the rectangular design space coincides with the envelope that completely surrounds the extremities of the shape.

In Fig. 2, when $\psi_I = \psi_A = \lambda = 1$ the rectangular envelope is completely filled. When $\lambda = 1$ and $\psi_I = \psi_A < 1$, the envelope $B \times H$ is filled in direct proportion to the shape transformers ψ_I and ψ_A . This is illustrated by the cross-sections placed on the diagonal line in Fig. 2.

The domain between curves 1 and 2 can be split into two regions, namely efficient and inefficient regions. Cross-sectional shapes where material is away from the neutral axis lie in the efficient region, where $1 < \lambda < 3$. Examples of shapes that partially fill the envelope and lie in the efficient region are I- and T-sections. Hollow rectangular sections also lie in the efficient region. A number of shapes are illustrated in Fig. 2. When the majority of material is near to the neutral axis, $0 < \lambda < 1$, the cross-sectional shapes lie in the inefficient region. Examples of cross-sectional shapes that occupy the inefficient region are shown in Fig. 2.

In Fig. 3, the equivalent curves for curves 1 and 2 in Fig. 2 are shown for different classes of shape. For elliptical cross-sections, values of ψ_A and ψ_I are less than unity, with their maxima at $\pi/4$ and $3\pi/16$ respectively for

the solid shape, as shown in Table 2. These maximum values are shown in Fig. 3 at point A. Curve 3 is the limiting curve for all elliptical shapes that are hollow, but with material close to the top and bottom of the outer surfaces. When the material is on the outer side edges, the efficiency of the beam in bending is described by curve 4.

When the envelope is square, rather than rectangular, $B = H$, the limiting curves in the envelope efficiency map move from curves 1 and 3 for rectangular and elliptical shapes to curves 1s and 3s respectively. Since the domain within the limiting curves is reduced, the range of λ is also reduced as shown in Table 2. For example, for rectangular sections the efficient region is when $1 < \lambda < 3$, whereas for square sections $1 < \lambda < 2$.

Similar to curves 1 to 4, curves are illustrated for triangular and lozenge-shaped cross-sections. It is emphasized that none of these shapes has a performance or efficiency that lies outside the boundary described by curves 1 and 2. Analogous to the efficient and inefficient regions defined for rectangular shapes, each domain for each shape class can be subdivided into two regions. For example, a triangle has an efficient section when $2/3 < \lambda < 2$, and an inefficient section when $0 < \lambda < 2/3$.

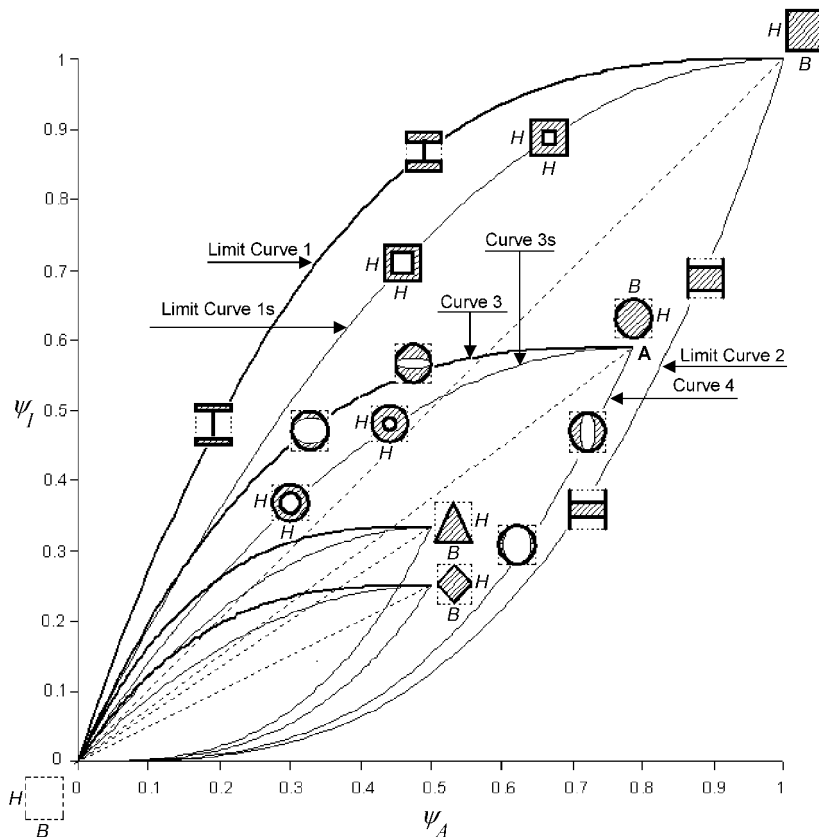


Fig. 3 Efficiency maps for different shapes. For the same envelope $B \times H$, the shape domain of the rectangle encloses any other domain (ellipse, triangle, lozenge)

5 GEOMETRIC CONDITIONS FOR OPTIMIZING STIFFNESS AND MASS

The performance criterion p/p_0 , given by equation (7) represents a means of defining the efficiency of a beam subjected to bending, i.e. maximizing the beam stiffness while minimizing the mass. The ratio p/p_0 is expressed in terms of the two geometric shape transformers ψ_A and ψ_I . These transformers also represent, for a given material, the relative stiffness and mass of the cross-section respectively. Consequently, as will be illustrated later, optimization of the mass for a given stiffness (related to ψ_I) means changing the geometric transformer ψ_A . Similarly, improving the stiffness for a given mass involves retaining ψ_A at a constant value and increasing ψ_I . In the following, the geometric conditions that arise for given stiffness and mass requirements are explored.

5.1 Minimization of mass

The envelope efficiency map shown in Fig. 3 illustrates efficient and inefficient regions for cross-section shapes that are bounded by the envelope B and H . For a given stiffness requirement, e.g. $\psi_I = 0.7$, minimization of the mass requires lower values of ψ_A . An example is shown in Fig. 4 for I-section beams and hollow box-sections. The best path for minimizing the mass for a given stiffness is from point R to A. It has already been shown that in bending stiffness design there are no possible solutions for values of

ψ_A less than that at point A in Fig. 4. At intermediate values of ψ_A between points R and A there are many shapes that can provide the stiffness requirement. Furthermore, if $\psi_I = 0.7$ represents the desired minimum stiffness, the cross-sectional shapes that lie in the shaded area above points R and A and the limit curve 1 also provide an efficiency, λ , greater than at point R in Fig. 4.

Further examples of minimization of mass for a given stiffness requirement are illustrated in Fig. 5. One design scenario is to consider reducing the mass of a solid circular section. Values of ψ_I and ψ_A for this section correspond to point E in Fig. 5. For a given stiffness (e.g. $\psi_I = 0.59$), minimizing mass requires exploring shapes that lie along path E to ERI. There are many shapes that occupy the design space $B \times H$. For simplicity, H- and I-sections that lie along path E to ERI are considered. Along the line E–W–ERI the rectangular section equivalent to the solid elliptical section that yields $\psi_I = 0.59$ has dimensions that satisfy

$$\frac{b}{B} \left(\frac{h}{H} \right)^3 = 0.411 \quad (8)$$

This is also illustrated in Table 3. When $b = 0$ and $h < H$, the idealized I-section with $\psi_I = 0.59$ lies on curve 1 in Fig. 5. The corresponding value of h/H for this condition is 0.743, as shown in Table 3. The variation in the thickness, i.e. the ratio b/B and h/H , for box and I-sections that lie along path W to ERI is given by equation (8) and is shown in Fig. 6.

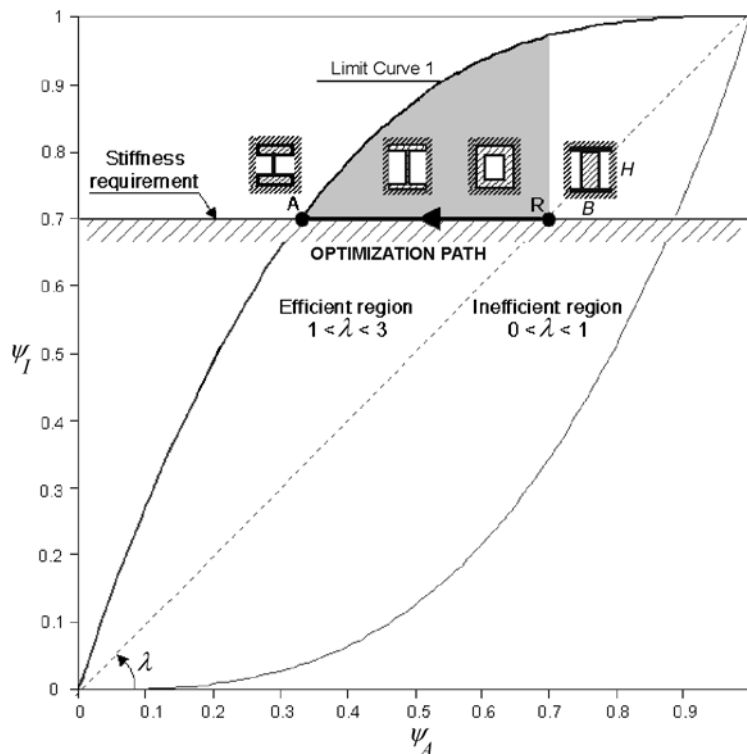


Fig. 4 Optimization path in an efficiency map. Only shapes above the stiffness line are selectable. However, the best optimization path is from R to A

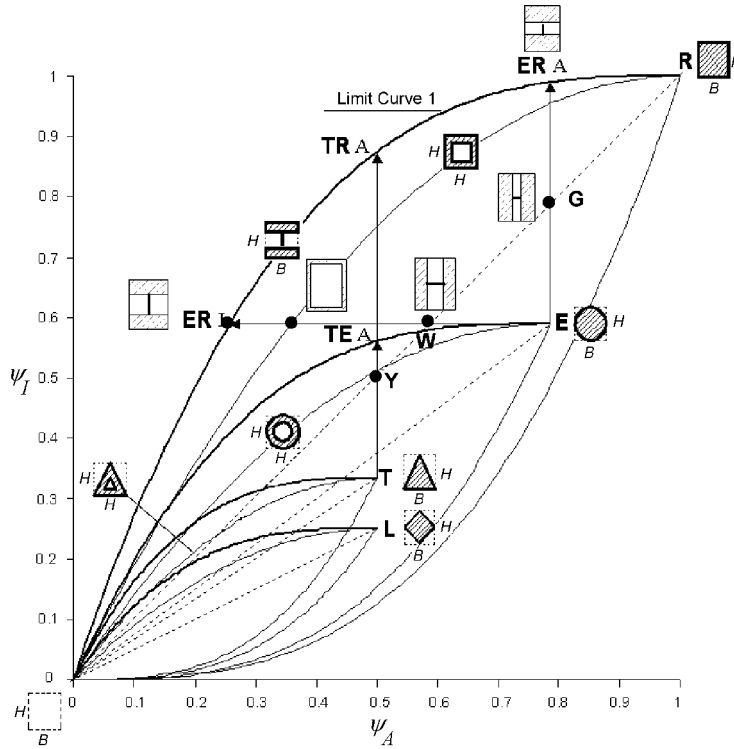


Fig. 5 Optimization paths for given ψ_I and ψ_A

Table 3 For a given ψ_I stiffness requirement (i.e. solid section on the first row), the above geometric conditions allow the efficiency of hollow sections (first column) in a fixed envelope $B \times H$ to be improved

| Geometric conditions to select and optimise hollow sections in a fixed envelope | ψ_I requirement of solid shape | | |
|---|--|--|--|
| | | | |
| | $\psi_I = \frac{3\pi}{16}$ | $\psi_I = \frac{1}{3}$ | $\psi_I = \frac{1}{4}$ |
| | $\frac{b}{B} \left(\frac{h}{H} \right)^3 = 0.411$ | $\frac{b}{B} \left(\frac{h}{H} \right)^3 = 0.6$ | $\frac{b}{B} \left(\frac{h}{H} \right)^3 = 0.75$ |
| | $\frac{h}{H} = 0.743$ | $\frac{h}{H} = 0.874$ | $\frac{h}{H} = 0.909$ |
| | | $\frac{b}{B} \left(\frac{h}{H} \right)^3 = 0.433$ | $\frac{b}{B} \left(\frac{h}{H} \right)^3 = 0.575$ |

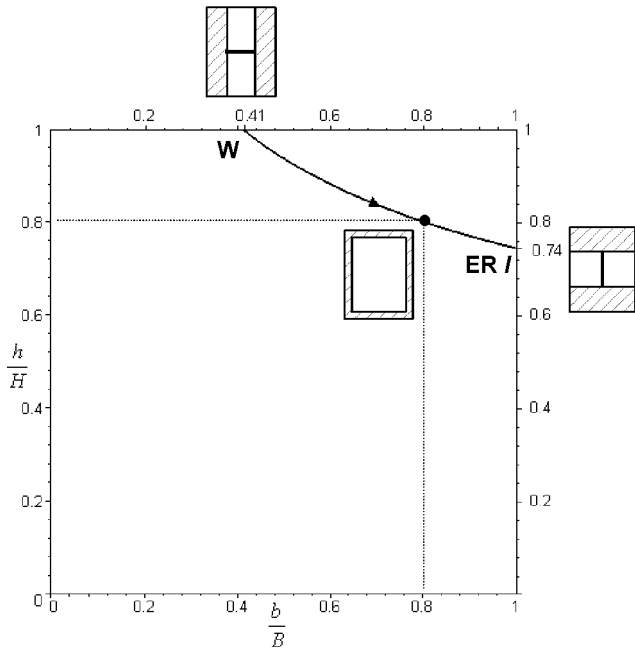


Fig. 6 Variation in beam dimensions for a given $\psi_l = 3/16\pi = 0.059$

5.2 Maximizing stiffness

For a given mass, the bending stiffness can be increased by moving along a vertical line on the envelope efficiency map. Several examples are shown in Fig. 5. By moving along the line E–G–ERA in Fig. 5 with $\psi_A = \pi/4$, various shapes occupying the design space can be chosen that improve the stiffness. Again for simplicity, box and I-sections are examined. As shown in Table 4, those sections that provide the same ψ_A as for an elliptical solid section have dimensions that satisfy

$$\frac{b h}{B H} = 0.215 \tag{9}$$

The idealized I-section with $b=0$ and $\psi_A = \pi/4$ lies on curve 1 in Fig. 5 at point ERA. The corresponding value of h/H is 0.215 (see Table 4). The variation in the ratios of b/B and h/H that corresponds to path G to ERA is given by equation (9) and is shown in Fig. 7.

This example can be extended to consider other shapes in a rectangular design space $B \times H$. Point T in Fig. 5 represents the best performance for a solid triangular

Table 4 For a given ψ_A requirement (solid section on the first row), the above geometric conditions allow the efficiency of hollow sections (first column) in a fixed envelope $B \times H$ to be improved

| Geometric conditions to select and optimise hollow sections in a fixed envelope | ψ_A requirement of solid shape | | |
|---|-------------------------------------|---------------------------|---------------------------|
| | | | |
| | $\psi_A = \frac{\pi}{4}$ | $\psi_A = \frac{1}{2}$ | $\psi_A = \frac{1}{2}$ |
| | $\frac{b h}{B H} = 0.215$ | $\frac{b h}{B H} = 0.5$ | $\frac{b h}{B H} = 0.5$ |
| | $\frac{h}{H} = 0.215$ | $\frac{h}{H} = 0.5$ | $\frac{h}{H} = 0.5$ |
| | | $\frac{b h}{B H} = 0.363$ | $\frac{b h}{B H} = 0.363$ |

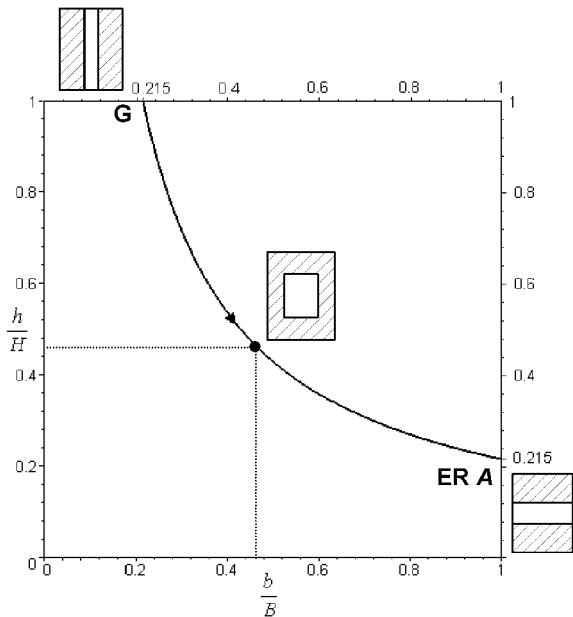


Fig. 7 Variation in beam dimensions for a given $\psi_A = \pi/4 = 0.785$

cross-section $\psi_A = 0.5$ and $\psi_I = 1/3$ (see Table 2). Assuming a given mass with $\psi_A = 0.5$, the solid triangle can be replaced by a more efficient shape, such as a hollow ellipse, at point TEA, or even better, an idealized box or I-section at TRA. The geometric conditions for equivalent rectangular shapes for solid ellipse, triangular and lozenge sections are shown in Table 4.

6 APPLICATIONS OF THE ENVELOPE EFFICIENCY MAP

The envelope efficiency map provides an effective means of determining which cross-sectional shapes are the most efficient in bending stiffness design. In this section, two applications of the map are considered:

1. The efficiency limits of practical steel cross-sections are explored.
2. The efficiency of multilayered material systems is considered.

6.1 Efficiency of practical cross-sectional shapes

Standard structural elements are manufactured to be suitable for different loading and operating conditions. In this section, only the mass efficiency in bending stiffness design is considered. Furthermore, standard cross-sections generally have different envelope sizes, and consequently the envelope efficiency map cannot be used to compare directly the structural performance. However, the map can be used to examine the practical limits imposed by current

manufacturing constraints on the shape transformers of the cross-sections.

The shape properties, ψ_A and ψ_I , of steel cross-sections available on the market are shown on the envelope efficiency map in Fig. 8. The structures considered are I-shapes of different typologies (IPE, HEA, HEB, INP), C shapes (UPN), tubes and boxes. The data for these improved sections are not very scattered, but they group together close to the limit curve 1. For I-sections their efficiency cannot achieve that provided by an idealized I-section with $b = 0$, since the web thickness has to be designed to avoid buckling.

Hollow circular sections (or tubes) lie on a curve that lies within the limit curve 3 for circular sections. Circular sections with variable wall thickness are generally impracticable to manufacture.

The empirical limits of λ for the various shapes in bending stiffness design are: 2.32 for HEA, 2.25 for HEB, 2.08 for IPE, 1.92 for IPN, 1.82 for UPN, 1.94 for square tubes and 1.46 for circular tubes. It is evident that these limits refer only to the shape properties of sections, and the contribution of the envelope sizes to the stiffness of the cross-section is not considered on the envelope efficiency map in Fig. 8.

6.2 Efficiency of multilayered systems

Multilayered systems are structures that contain different combinations of materials placed in layers. In this section, the efficiency envelope map is used to explain the properties and the performance of multilayered systems.

Many authors have developed analytical solutions for simple layered systems. However, the relationship between layer location and stiffness has only been recently examined [10]. Smith and Partridge [10] explored the flexural stiffness of planar multilayered systems that contain two materials: titanium alloy IMI 834 and Ti-6Al-4V metal matrix composite (MMC). The results of their analysis are shown Fig. 9, where flexural modulus or bending stiffness is shown as a function of density. All the possible layered materials based on the two-material systems Ti-MMC and Ti-834 are located in a domain defined by curves 1 and 2.

The envelope efficiency map shown in Fig. 3 can be related directly to the results shown in Fig. 9 for the layered system. The efficiency map corresponds to a single material subjected to bending. The efficiency of the cross-section depends on its second moment of area, I , and the area occupied by the material.

Now, consider a multilayered system consisting of two materials with Young's moduli E_1 and E_2 and densities ρ_1 and ρ_2 . The performance of the combined system will depend on the relative values of the moduli and densities. Each material contributes to the total performance of the envelope, $B \times H$. If h is the height of the envelope filled by material 1, then $H - h$ is the height filled by material 2.

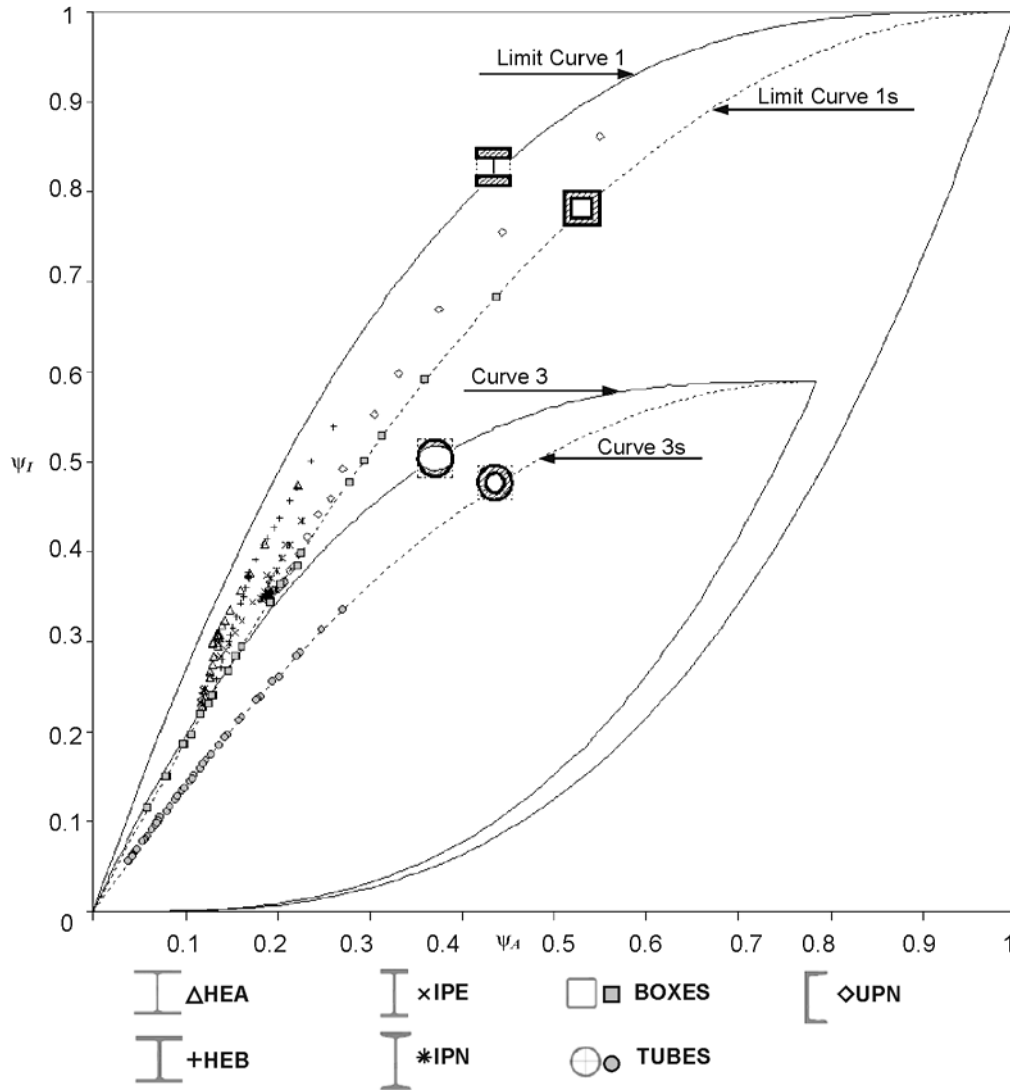


Fig. 8 Steel cross-sections available in the market (data source: EURONORM 53-62; 19-57; 5679-73). Note that the aim of this plot is to show only the limits of the shape transformers, and thus the effect of the envelope sizes on the efficiency is neglected

Therefore, the total flexural modulus, E_T and density, ρ_T of the layered system are given by

$$E_T BH^3 = Bh^3 E_1 + B(H^3 - h^3) E_2 \quad (10)$$

$$\rho_T BH = Bh\rho_1 + B(H - h)\rho_2 \quad (11)$$

Dividing equations (10) and (11) by BH^3 and BH respectively and using the expressions of the shape transformers given in Table 2 gives

$$E_T = \psi_I E_1 + (1 - \psi_I) E_2 \quad (12)$$

$$\rho_T = \psi_A \rho_1 + (1 - \psi_A) \rho_2 \quad (13)$$

The limits of the shape transformers ψ_A and ψ_I are given in Table 2 and illustrated in Fig. 4. Using the properties for

Ti-MMC ($E_1 = 204$ GPa, $\rho_1 = 4.38$ mg/m³) and Ti-834 ($E_2 = 114$ GPa, $\rho_2 = 4.57$ mg/m³) together with equations (10) and (11), gives the results in Fig. 9.

Note that when $\psi_A = \psi_I = \lambda = 1$ the layered system is all Ti-MMC with $E_T = E_1$ and $\rho_T = \rho_1$. Similarly, when $\psi_A = \psi_I = 0$, the layered system is all Ti-834. These extreme values are illustrated in Fig. 9. Curves 1 and 2 in Fig. 9 represent a symmetric layered system with Ti-MMC on the upper and lower surfaces (curve 2), or with Ti-834 on the upper and lower surface. As explained in this paper, all the possible multilayered systems lie within the domain bounded by the limiting curves. Smith and Partridge explored alternative symmetric and asymmetric systems and found them to be within curves 1 and 2. The envelope efficiency map introduced in this paper illustrates that many other cross-sectional shapes other than simple layered

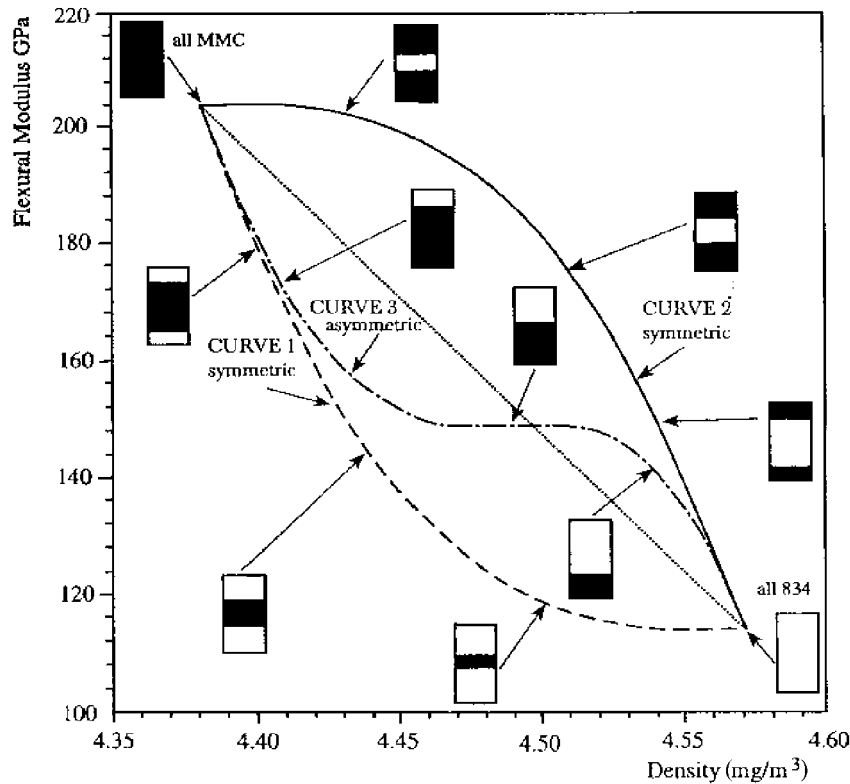


Fig. 9 Flexural stiffness of two- and three-layer system using Ti-MMC and Ti-834 (from Smith and Partridge [10])

systems can be explored and the stiffness and density of the system determined simply from equations (12) and (13).

7 SCALING OF THE CROSS-SECTION

This paper has so far examined the structural efficiency of cross-sections that are not scaled. The cross-sectional shapes have been considered to have the same envelope surrounding the shape as shown in Fig. 1. The findings provided in this work can be related to earlier papers [8, 9] which considered the arbitrary scaling of the envelopes enclosing the shapes. Arbitrary scaling means that a cross-section is enlarged or contracted in any direction including widthwise, heightwise, proportionally and in any other direction. The reason why a cross-section may be constrained to certain directions of scaling is that practical design cases often contain geometrical constraints on the design space. Cross-sections need to be scaled in size in order to meet a particular stiffness requirement with a different material or to meet a changed stiffness requirement with same or a different material.

Consider four cross-sections of the same material, D_0 to D_3 , shown in Fig. 10. Here, D_0 is a rectangular cross-sectional shape with shape transformers $\psi_A = 1$ and $\psi_I = 1$ and sizes of the envelope B_0 and H_0 . Cross-section D_1 is a hollow section that lies in the efficient region in Fig. 2. Since

D_0 and D_1 are not scaled, the dimensions of the hollow section are H_0 and B_0 , while h_0 and b_0 are the internal dimensions. Cross-sections D_2 and D_3 are arbitrarily scaled cross-sections derived from D_1 . The relative changes in widths B and b and heights H and h are described by two linear multipliers $u = B/B_0 = b/b_0$ and $v = H/H_0 = h/h_0$.

Consider now the position of the rectangle D_0 on the envelope efficiency map shown in Fig. 11. If a shape with $\psi_A = 0.43$ and $\psi_I = 0.81$ is selected for envelope D_0 , $B_0 \times H_0$, then D_0 moves to D_1 with coordinates (ψ_A, ψ_I) , as shown by the arrow $D_0 D_1$ in Fig. 11. Cross-section D_1 is a structure that cannot provide the same stiffness as D_0 . However, if cross-section D_1 is scaled to D_2 , the stiffness, k_0 , provided by D_0 can be made the same as that for D_2 , i.e. $k[D_2] = k_0[D_0]$. It can be shown [9] that, in stiffness design, the cross-sections meet the same requirement for the following conditions

$$\frac{k}{k_0} = uv^3\psi_I = 1 \quad (14)$$

Consequently, if $u = 0.5$ is chosen, equation (14) can be used to determine the appropriate value of v that satisfies the stiffness requirement. Note that ψ_I and ψ_A correspond to the value of the shape transformer for cross-section D_1 with $\psi_A = 0.43$ and $\psi_I = 0.81$. The values of v that satisfies equation (14) is 1.26. Another example is to select $u = 2$,

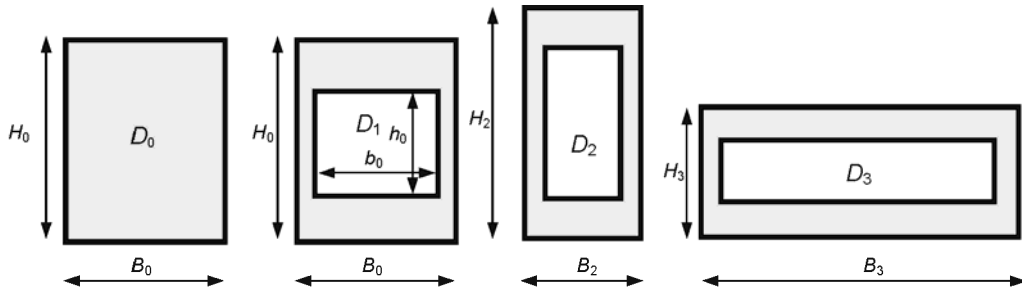


Fig. 10 Changes in cross-sectional shapes and different scaling of the envelope

and then using equation (14) gives $v = 0.79$. The solution corresponds to cross-section D_3 .

When cross-section D_1 is scaled according to the stiffness requirement given by equation (14), then point D_1 in Fig. 11 moves along arrow D_1D_2 to coordinate $D_2 (\psi_A^*, \psi_I^*)$ given by

$$\begin{aligned} \psi_I^* &= uv^3\psi_I \\ \psi_A^* &= uv\psi_A \end{aligned} \tag{15}$$

Figure 11 shows the effect of scaling on boundaries curves 1 and 2 of the envelope associated with D_0 for two cases. In the first case, all the shapes within curves 1 and 2 are rescaled to meet the stiffness requirement with $u = 0.5$ and

$v = 1.26$. The shapes enclosed by limiting curves 1 and 2 are now enclosed by curves 3 and 4. In the second case, $u = 2$ and $v = 0.79$ and any point of limiting curves 1 and 2 moves to the respective point of curves 5 and 6. In this case the cross-sectional shape D_1 moves to D_3 . In the first case the effect of scaling is such that, since $v > 1$, the height of D_2 is increased and moves to the left with a consequent improvement in efficiency. On the other hand, when $v < 1$, this causes the curves to move to the right towards less efficient cross-sections.

In practice, wide flanges on I- and T-sections are not fully effective in carrying bending loads. In cases where wide sections are needed on account of space constraints, it is generally better to use box and channel sections rather than I- and T-sections respectively.

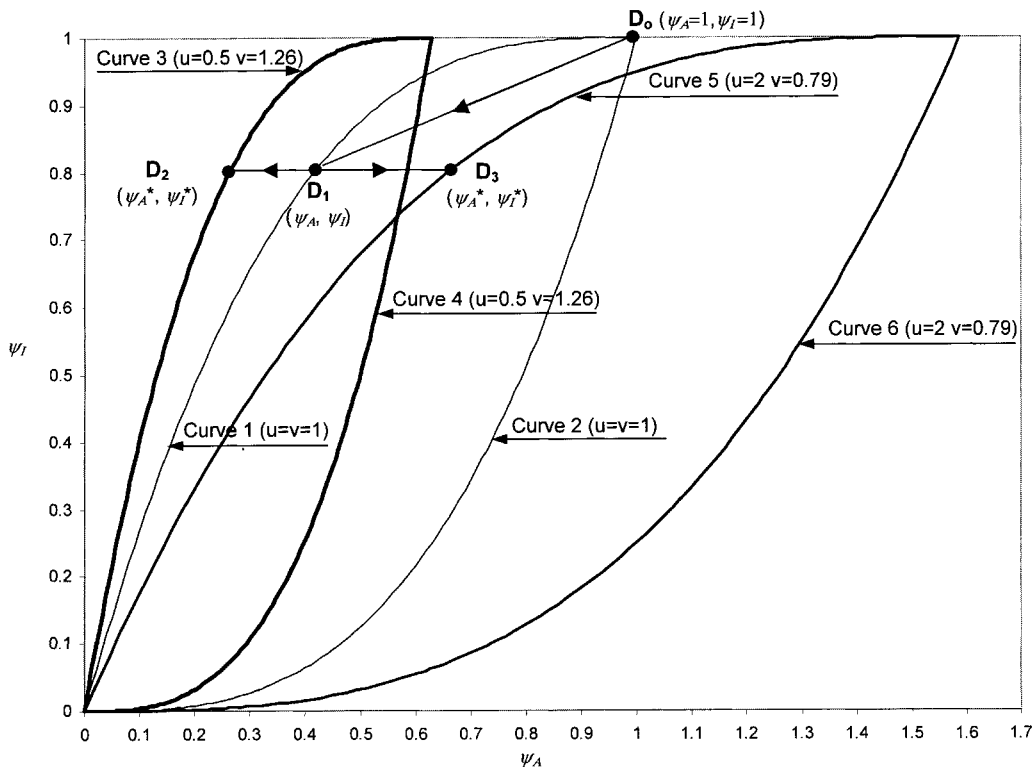


Fig. 11 Effect of scaling the envelope on the efficiency map

8 COST MEASURE

The envelope efficiency map can be used to select cross-sections that maximize the stiffness per unit cost. In Fig. 2, ψ_I is plotted against ψ_A : ψ_I is the shape transformer of the second moment of area and is related to the stiffness, k , of a structural component; ψ_A is the shape transformer of the area and therefore is directly related to the mass, m . If C is the cost per unit mass, then the cost of a component is Cm .

Using the definition of the shape transformer [equation (4)], the cost Cm of a structural component with length L and density ρ is given by $Cm = C\rho AL = C\rho\psi_A A_D L$. Therefore, for a given material, $C\psi_A$ represents the cost measure of a beam per unit volume, i.e. $A_D L = 1$. Replacing ψ_A with $C\psi_A$ on the horizontal axis of the envelope efficiency map shown in Fig. 2 allows the cost of a structural member to be evaluated for a bending stiffness requirement.

9 CONCLUDING REMARKS

The structural efficiency of beams subjected to bending has been the focus of this paper. The performance criterion for the beam is to make it as stiff as possible while reducing mass. It has been shown that there are many cross-sectional shapes whose main dimensions touch the boundary of a rectangular design space, and all these shapes lie within two limit curves. The curves are functions of two parameters, ψ_A and ψ_I , called shape transformers, which represent the area and second moment of area of a cross-sectional shape relative to its surrounding envelope.

The analysis presented in this paper is restricted to beams of elastic material. Similar approaches could be adopted for other loading conditions and also for elastic-plastic material

behaviour. The efficiency map provided in this paper gives insight into the performance of structures.

REFERENCES

- 1 Cox, H. L. *The Design of Structures of Least Weight*, 1965 (Pergamon Press, Oxford).
- 2 Shanley, F. R. *Weight-Strength Analysis of Aircraft Structures*, 2nd edition, 1960 (Dover, New York).
- 3 Parkhouse, J. G. Structuring a process of material dilution. In *Proceedings of 3rd International Conference on Space Structures* (Ed. H. Nooshin), 1984, pp. 367–374 (Elsevier Applied Science Publishers, Oxford).
- 4 Parkhouse, J. G. and Sepangi, H. R. *Macromaterials. Conference Proceedings* (Ed. F. N. Spon), 1993, pp. 3–13 (Garas Armer and Clarke, London).
- 5 Ashby, M. F. *Materials and shape. Acta Metall. Mater.*, 1991, **39**(6), 1025–1039.
- 6 Ashby, M. F. *Materials Selection in Mechanical Design*, 1st edition, 1992 (Pergamon Press, Oxford).
- 7 Burgess, S. C. Shape factors and material indices for dimensionally constrained structures. Part 1: beams. *Proc. Instn Mech. Engrs, Part C: J. Mechanical Engineering Science*, 1998, **212**(C2), 129–140.
- 8 Pasini, D., Burgess, S. C. and Smith, D. J. Performance indices for arbitrarily scaled rectangular cross-sections in bending stiffness design. *Proc. Instn Mech. Engrs, Part L: J. Materials: Design and Applications*, 2002, **216**, 1–13.
- 9 Pasini, D., Smith, D. J. and Burgess, S. C. Selection of arbitrarily scaled cross-sections in bending stiffness design. *Proc. Instn Mech. Engrs, Part L: J. Materials: Design and Applications*, 2003, **217**(2), 113–125.
- 10 Smith, D. J. and Partridge, P. G. Flexural stiffness envelopes for planar system containing two dissimilar materials. *Proc. Instn Mech. Engrs, Part L: J. Materials: Design and Applications*, 1999, **213**, 1–20.
- 11 Pasini, D., Burgess, S. C. and Smith, D. J. A method of selection for large scaled structures. ASME 2002 Design Engineering Conference, Montreal, Canada, 2002.